A stochastic hazard assessment for Australia based on an external perspective

Andreas Schäfer[1,2] & James Daniell[1,3]
[1] Geophysical Institute & Center for Disaster Management and Risk Reduction Technology (CEDIM), Karlsruhe Institute of Technology (KIT), Hertzstrasse 16, 76187, Karlsruhe, Germany.
[2] Ludwig-Maximilians-Universität München, Theresienstraße 41, 80333 Munich, Germany
[3] John Monash Scholar, The General Sir John Monash Foundation, Level 5, 30 Collins Street, Melbourne, Victoria, Australia 3000.

E-Mail: aschaefer.engineering@gmail.com

Abstract:

Australia is in a unique position globally being a continent where Mw7.0 events can occur in the Craton, and potentially similar large events in the non-Craton areas, however only a recorded history of around 150-200 years or less exists in most locations. Although a low-moderate seismicity country, many locations have already experienced damaging earthquakes.

The recent earthquake hazard maps in Australia are discussed and compared with some other nations. Earthquake hazard maps in locations such as France where over 2000 years of data have provided a smoother view of seismicity are representative of what a seismic hazard map can be when a significant event record has occurred. For comparison, simplified hazard maps of these locations are introduced using the same amount of data as Australia has available.

Using a combined model of cluster analysis, smooth seismicity, seismic source zones and ground motion prediction equations an alternative stochastic Australian hazard model has been built up. Problems such as the short earthquake history and the lack of larger events mean that the Australia hazard model requires as much data as possible, and not simply an instrumental catalogue from the last few decades.

Keywords: Australia hazard map, historical comparison, smooth seismicity, stochastic analysis

1. Introduction

The development of hazard maps is an essential part of handling and quantifying the threats of natural hazards. Especially in terms of earthquakes it is rather difficult to build sophisticated hazard maps because both the process and the occurrence pattern of earthquakes are not well enough understood. In addition to this, the related data to model these maps are often limited and in most of the cases, as far as science knows, not enough to model complete earthquake cycles. Furthermore, there are often gaps in data, or misunderstood information; thus the general uncertainty of especially historic and paleoseismic earthquakes is rather large. For example, the 2011 Tohoku earthquake occurred along an active subduction zone, known to be able to generate very large earthquakes, but that the earthquake reached about magnitude 9.1 was not expected based on the official Japanese hazard map and scientific publications. Afterwards, it was found out that there have been actual historical remarks about large tsunami waves rolling deep into the land, which could have been directly related to earthquakes with a respective magnitude [Stein et al. 2012]. Also taking the 2010-2011 earthquake sequence in New Zealand, in September 2010, the Mw = 7.1 earthquake hit the northern Canterbury plains, causing no fatalities, but a reasonable amount of damage in surrounding regions, including the town of Christchurch. Only several months later, in February 2011, a Mw= 6.3 earthquake occurred along a previously unknown fault close to the city of Christchurch, causing tremendous damage and approximately 186 fatalities. Multiple in-depth mapping projects in the years before the earthquakes didn't show any sign that there might be a major fault line, thus indicating that even detailed geologic investigations might not identify all major fault lines hidden in the earth's crust [Elliot et al., 2012]. Another example arises from the eastern US, where in 2012 the Mw=5.9 Virginia intraplate earthquake occurred which, based on the historic knowledge, was not supposed to be possible at that location. There was a recorded history of earthquakes of about 400 years, with no indication of any event larger than about Mw=4. This demonstrated that even 400 years is not enough to cover seismic cycles of low-activity intraplate regions. Faults have been mapped and are well-known in that region, but their actual capabilities of maximum magnitude events seem to be highly questionable [Horton, 2012].

Australia faces similar problems to those listed above. With a recorded history of approximately 175 years for populated regions, and about 60 years of history for about the whole continent, it is extremely difficult to model a complete representation of earthquake hazard, since seismic cycles especially in an intraplate environment tend to last hundreds or thousands of years. Events such as the 1989 Newcastle earthquake show that there is an inherent threat to Australia's population. Since the late 1970s, earthquake hazard maps have been developed and published both for civil security purposes as well as for the official earthquake load code AS1170.4. The latest version of the Australian hazard map has been published in 2012 and undergoes a review every 5 years [Burbidge, 2012]. This hazard map will be examined and reviewed in Section 2, showing key improvements with respect to older versions, but also indicating possible elements for future advancement. In Section 3, a comparison of simplified hazard maps is shown for continental Western Europe and Turkey, using different time periods of data. This comparison will indicate how strongly the effect of the length of recorded earthquake history can affect the results of earthquake hazard maps. An alternative approach for modelling an Australian hazard map is given in Section 4 using smooth seismicity and clustering techniques. In Section 5, the results are analyzed and compared with the existing hazard map of 2012.

2. Review of the existing Australian hazard maps

For the new Australian hazard map, a combined catalogue has been established, merged out of several general and local catalogues, and afterwards declustered by applying both an

automatic and manual approach. The source model consists out of three layers; one layer on a sub-national level, a regional source zonation and a set of hotspots. With these zones a new Gutenberg-Richter algorithm has been applied to calculate the earthquake frequency. The hypothetical maximum magnitude per location has been inferred from neo-tectonic domains and is thus one of the first hazard maps applying such a semi-quantitative measure. In addition, two new ground motion prediction equations have been introduced to calculate local ground accelerations. The final hazard map is then a superposition of the three layers of the source model. In the end a set of hazard maps has been assembled from the different hazard layers with respective source parameters for multiple reoccurrence periods. Figure 4 shows multiple excerpts from the original report, containing an overview of the data sources, magnitude changes, regional source zones and one of the final earthquake hazard maps for a 500 year return period.

2.1 Model

The applied methodology follows in general the standard procedure of probabilistic seismic hazard assessment, but with slight deviations. As a first step, in total 5 earthquake catalogues have been combined, partially covering different parts of Australia. A special focus has been on the conversion of magnitudes. As a result of different measurements and calculation formulae to acquire local magnitudes during the last decades, an intense magnitude scale analysis has been undertaken. Local magnitudes have been adjusted, showing that remote locations tend to be overestimated previously. Afterwards, a general conversion to moment magnitude has been preferred for the later application of ground motion prediction equations. The data have been declustered using an expert opinion technique and a mixture of three window methods adjusted to the Australian setting both forward and backward in time.

The seismic source zonation is based on three layers. The first layer represents the background seismicity, dividing Australia into a total of four zones. The mainland is divided into east and west, representing cratonic and non-cratonic tectonic domains, the third zone is non-cratonic Tasmania, while the fourth zone is the extended continental crust of Australia's passive margin. The second layer has regional zones representing a zone setup based on a smooth seismicity approach and the third layer is made of a couple of small locations which are considered to be hotspots of very local activity. In addition, three offshore zones have been considered north of Australia in terms of very large earthquakes. In terms of the Gutenberg-Richter relation, an alternative approach has been applied by combining four different methods of calculating earthquake reoccurrence. At first, the two standard ways of calculating the Gutenberg-Richter relation have been applied; least-squares and maximum likelihood. In addition, a gap method has been applied which considers only magnitude bins which are not further apart than 0.3 and a method where the *b*-values were fixed to b=1 and only the *a*-value was adjusted to the data. In the end, a combination logic was applied by checking whether the *b*-value was within a boundary of 0.82 and 1.15. The gap method was first considered, followed by the maximum-likelihood and the standard least squares; if none of them lead to satisfying results, the fixed b-value approach was applied. The completeness magnitude was achieved via standard methods. Unique about this hazard map was to consider seismo-tectonic features to determine the maximum magnitude. A back calculation from fault data, where earthquake rupture scraps have been analysed, was used to gain information about historic maximum magnitudes, or paleo-seismic maximum magnitudes. This led in total to a maximum magnitude ranging from 7.3 to 7.7 for the sub-national and regional zones, and 5.8 to 6.5 for the identified hotspot zones. Finally, the whole model was concluded with the application of multiple ground motion prediction equations. 11 equations have been considered to be useful for Australia, from which 5 have been chosen after multiple tests. Two of these equations have been developed for Australia and published during the last few years.

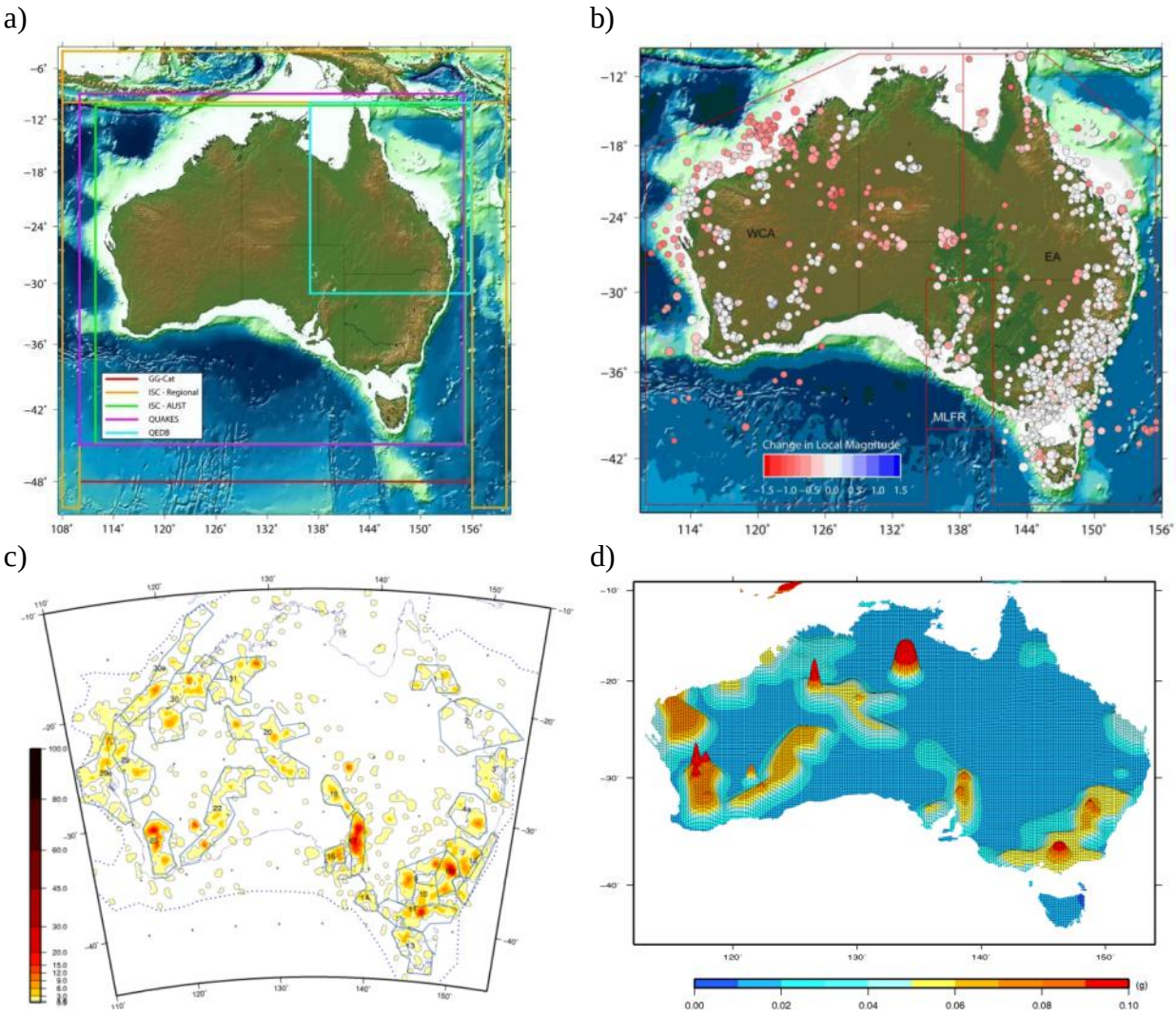

Figure 1: a) shows the spatial extent of the 5 implemented earthquake catalogues. b) the changes of local magnitudes after the reanalysis. c) smooth seismicity distribution and respective regional source zones. d) one of the final earthquake hazard maps, peak ground acceleration for a 500 year return period. [Burbidge et al. 2012]

2.2 Review

This new approach introduces a couple of good ideas into the general field of probabilistic hazard. At first, reviewing and adjusting the magnitudes of the dataset should be done more often for such projects. Showing the tremendous changes at some locations, especially remote locations can have a significant impact on later calculations. Introducing and merging multiple layers of source zones is also considered to be a promising technique in separating different domains of activity. But too small defined zones, especially for locations with a not well recorded or too short earthquake history, might bind the occurrence distribution of earthquakes too strongly. It neglects the option of earthquake and hotspot propagation and migration and hence, considering hotspot zones should be examined more critically, especially with a recorded history of only approximately 100 - 150 years. Counter-examples will be introduced in Section 3, introducing locations with better documented history, where large seismic provinces could have been misinterpreted by simply using the last century of data. Furthermore, setting boundaries on the Gutenberg-Richter relation prevents the model obtaining its own dynamics. Extreme results of the Gutenberg-Richter relation might simply be related to too small data in the respective zone. It might be useful, instead, to change the geometry of data acquisition. Nevertheless, the application of seismo-tectonic features to

determine the maximum magnitude is outstanding and currently the best option for locations with only a short recorded earthquake history. It does not necessarily mean that there will never be a larger event, but it at least sums up what can be inferred from geologic features. The 2012 Australian hazard map is an intelligent advance on older versions. It introduces various useful ideas which are quite promising. These should be further applied in future studies, such as the large-scale application of seismo-tectonic features to identify maximum magnitudes as well as the gap method to calculate the Gutenberg-Richter relation.

3. Time-period comparison of international hazard maps

In the following section, multiple simplified hazard maps are compared. The purpose of this comparison, in terms of Australian earthquake hazard, is to show how important it is to have a long recorded history of earthquakes and how to find possible solutions in designing and modelling hazard maps with insufficient data support. The chosen locations of interest for this comparison have been Continental Western Europe and Turkey. While Western Europe represents a tectonic environment similar to Australia in terms of earthquakes, Turkey shows the effect of data capping for high seismicity regions. For both locations about 1000 years of data are evaluated. The main data source of the Western European map was the SHARE database [AHEAD] until 2006 and for Turkey a combination of the EMEC Catalogue [Grünthal and Wahlström, 2012] until 2006 and data from the Northern California Earthquake Data Center [ANSS] from 2006 until 2013. All magnitudes have been converted into moment magnitudes. The catalogues have been declustered using the window method of Gardner and Knopoff [1974]. The simplified hazard maps have been modelled using the time-independent toolbox of Schaefer et al. [2014] applying a smooth seismicity approach. Here, a Gaussian distribution has been chosen with an average smoothing distance of 35 km applied to a 5x5 km grid. Gutenberg-Richter values have been calculated using a standard least-squares approach. Completeness has been estimated using an automatic algorithm.

	Max. Mw	**#events**	**b-value**	**a-value**	**Mw > 5.0**	**Mw > 6.0**
West EU 1000	6.7	1479	1.14	5.40	488	35.
West EU 1900	6.5	644	1.20	5.83	622	38
West EU 1960	6.0	262	1.33	6.30	409	19
1900 vs. 1000		43.54%			127.50%	109.75%
1960 vs. 1000		17.71%			83.54%	53.38%
	Max. Mw	**#events**	**b-value**	**a-value**	**Mw > 5.5**	**Mw > 7.5**
Turkey 1000	8.1	2522	1.05	5.94	1363	10
Turkey 1900	7.6	2328	1.02	5.84	1657	15
Turkey 1960	7.4	1915	0.97	5.58	1576	17
1900 vs. 1000		92.31%			121.55%	141.69%
1960 vs. 1000		75.93%			115.58%	164.83%

Table 1: Parameter results for Western Europe and Turkey, with calculated average number of events for Mw > 5.5 and Mw > 7.5 for a 1000 year period inferred from the Gutenberg-Richter values.

	4 - 4.5	**4.5 - 5**	**5 - 5.5**	**5.5 - 6**	**6 - 6.5**	**6.5 - 7**	**7 - 7.5**	**>7.5**
West EU 1000	1685	1648	1562	1482	1390	1364	1364	1364
West EU 1900	1900	1900	1900	1900	1900	1900	1900	1900
Turkey 1000	1971	1951	1912	1869	1511	1158	1002	1002
Turkey 1900	1971	1951	1915	1900	1900	1900	1900	1900

Table 2: Completeness periods for Western Europe and Turkey for datasets from the year 1000 and year 1900 until 2006 and 2013 respectively.

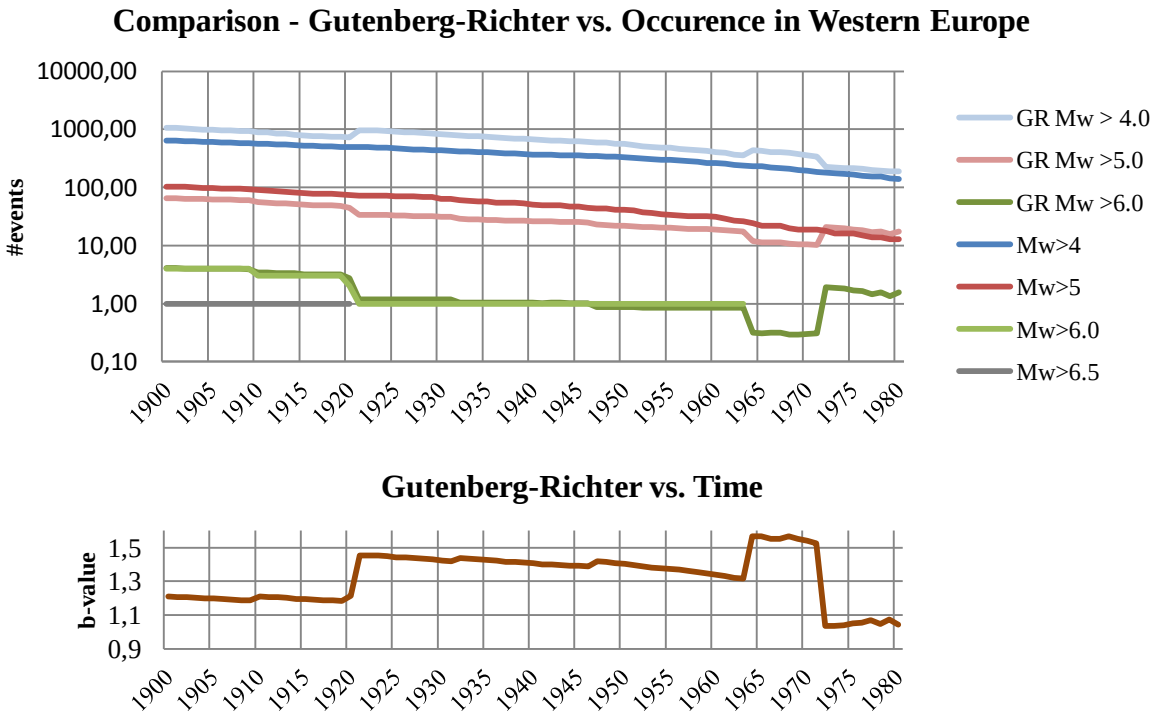

Figure 2: Shows a comparison of calculated number of events from the Gutenberg-Richter values vs. the actual occurrence during the estimation period for Western Europe. Each point represents a period of data starting from the denoted year in the x-axis (1900 1980) until 2006.

Two time periods have been examined; the whole dataset from year 1000 onwards and from 1900 until the present. For the purpose of this section, the year 1900 has been chosen with respect to the existing Australian data. In Australia, the earliest earthquake record dates back until about 1850, but the data are extremely sparse, accounting for a more complete cover of the Australian continent, it is assumed that the year 1900 can represent a respective time when the data coverage is complete enough to be compared to other regions with a larger record. In addition, 1960 can be seen as the year in Australia when most necessary earthquake magnitudes are about to be recorded. Thus, Table 2 shows the calculated completeness periods and Table 1 shows the resulting Gutenberg-Richter values and general parameters of the respective period.

Based on the resulting model parameters, various characteristics are shown in the table above. The effect of a longer time period in Turkey adds 194 additional historic events to the dataset from 1900 to 1000 and about 607 from 1960, which represents about 8% and 24% of the whole catalogue respectively. Consisting of mainly strong magnitude events, it leads to a consolidation of the Gutenberg-Richter relation, decreasing the theoretical number of a 1000 year statistics to about 70% and 55% for Mw> 7.5 and to about 80% and 85% for Mw > 5.5. It is similar for Western Europe for the period of 1900 with respect to the total catalogue, where 834 pre-1900 have been removed for the younger period and 1217 pre-1960 have been removed for 1960. For the oscillation using a longer data period is about ±20% and about the same for average magnitudes of Mw > 5.5. However, this is only marginal and within the error range for the period since 1900, thus, showing that for Western Europe the earthquake record of the last 100 years fits with the long-term average of earthquake activity in terms of frequency. But taking the period from 1960 indicates the opposite, with an extreme difference in the frequency of large magnitude events, shown in Figure 2, since no Mw>6 earthquake has been observed since the 1963 Mw=6.0 Ligurian Sea earthquake.

The period after 1960 seems to be covered more by low seismicity events than larger ones, decreasing the general hazard to about 65% for Mw > 5.5 and 40% for Mw>6.5. Choosing Mw > 7.5 and Mw > 6.5 respectively for Turkey and Europe is related to the general maximum magnitude observation, whilst for Western Europe extreme events are about Mw = 6.5 ± 0.5 and for Turkey Mw = 7.5 ± 0.5. In general, applying a longer period of data leads to a consolidation of the Gutenberg-Richter relation, because the seismic cycle can be captured more completely, which is also visible in the completeness information of the Turkish dataset, where at a magnitude of Mw>5 the completeness periods are influenced by the increased data range. Results of the Gutenberg-Richter relation are not extremely influenced as long as the major magnitude range is covered (e.g. [3.5, 6.5]). This can be seen for Western Europe in the difference for 1900 and 1960, for regions with a strong seismicity, e.g. for Turkey this effect is a lot weaker. Thus, Gutenberg-Richter relations calculated from longer time periods can be seen as more reliable.

Figures 3 and 4 show the resulting smooth seismicity maps for Western Europe and Turkey. Neglecting the absolute values of event density, the results have been normalized for visualisation purposes. By comparing maps from 1900 to maps from 1000, multiple locations which have been active during the last 1000 years are not indicated in the short-period maps. For example, the complete seismic field of central France is not even visible for Mw>5.0. Instead, smaller magnitudes Mw>4.0 occurred since 1900; thus it is necessary to infer locations of strong earthquakes via locations with weaker seismicity. It is similar for Turkey, where, for example, the whole field of the Eastern Anatolian Fault is not visible with earthquakes with Mw>6.0. On the other hand, inferring information of smaller magnitudes does not directly indicate locations of large earthquakes. Instead, a density correlation shows, that a large number of smaller earthquakes can also indicate a location of possible large events.

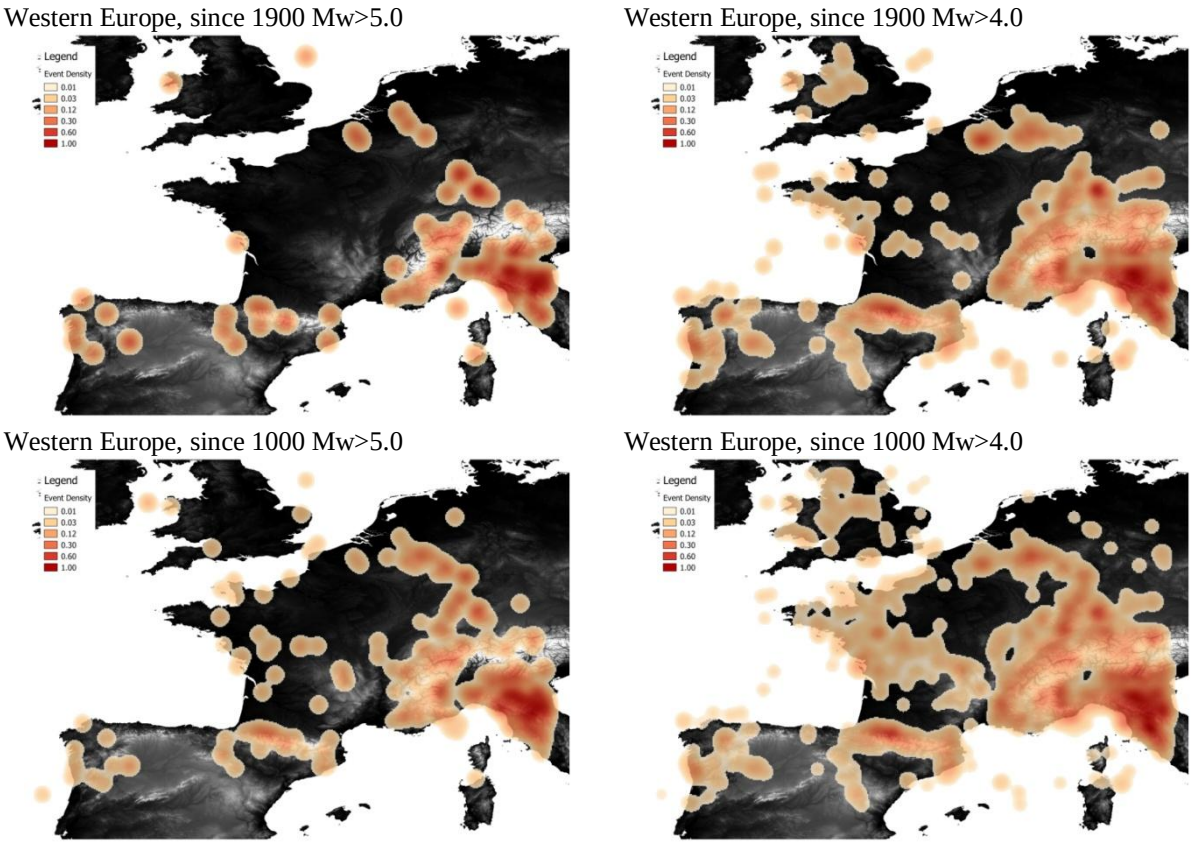

Figure 3: Comparison of different smooth seismicity maps for Western Europe, for periods since 1900 and 1000 showing the normalized event density per 5x5 km² grid point.

Turkey, since 1900 Mw>6.0

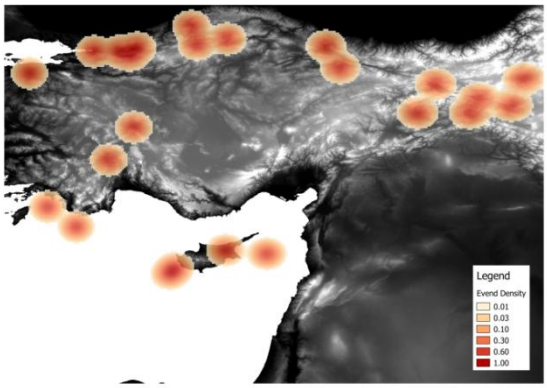

Turkey, since 1900 Mw>4.0

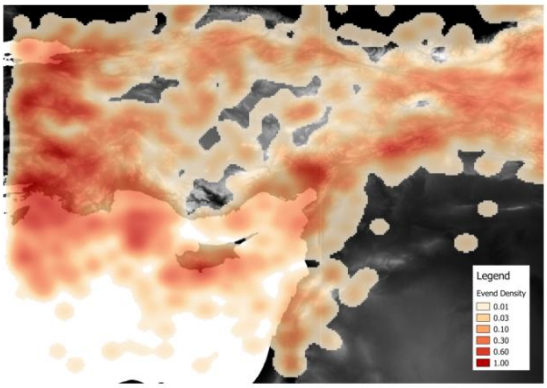

Turkey, since 1000 Mw>6.0

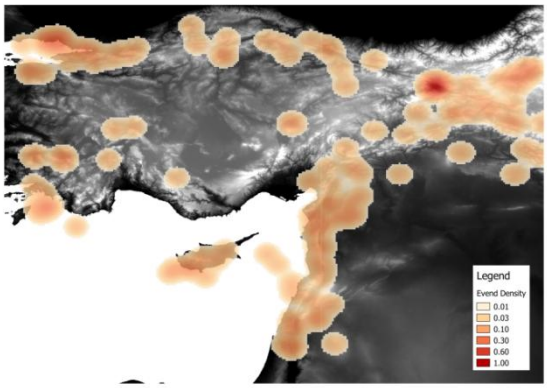

Turkey, since 1000 Mw>4.0

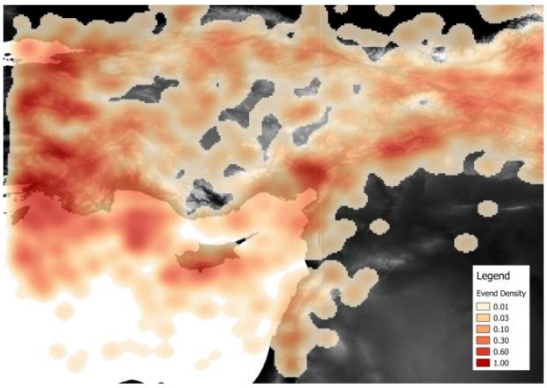

Figure 4: Comparison of different smooth seismicity maps for Turkey, for periods since 1900 and 1000 showing the normalized event density per 5x5 km² grid point.

In summary, having only a limited amount of data will lead to incomplete results for hazard map calculations. Inferring maximum magnitude information from only 100 years of recorded earthquake history will automatically lead to underestimations of the real activity, or even overestimation in case of the Albstadt earthquake sequence from 1900 onwards in South-West Germany. Furthermore, locations of strong earthquakes can be correlated with the density distribution of smaller events, as shown in Figure 3. For the estimation of Gutenberg-Richter parameters about 100 years of data are sufficient to obtain models within the acceptable error ranges, but additional data consolidate the results. Thus, the major problem of hazard maps modelled using only limited data will probably not hinder estimating earthquake frequencies, except in terms of earthquake distribution and the maximum magnitude estimation. With respect to the 2012 Australian hazard map, the field of maximum magnitude has been successfully applied by inferring the magnitudes from seismo-tectonic information.

4. Methodology for an alternative hazard map

To build an alternative approach for an Australian hazard map, the results of Section 2 and 3 have been analysed. Therefore the focus will be on the field of earthquake distribution, using low-magnitude background seismicity as proxy information for locations of larger earthquakes. This alternative hazard map follows the following modelling procedure:

1. Declustering of data via the window-method and the optics-method
2. Calculation of background seismicity distribution via optics-declustered data
3. Calculation of Gutenberg-Richter parameters via window-method declustered data and completeness magnitudes for each source zone
4. Calculation of stochastic datasets using a Monte-Carlo simulation
5. Application of intensity prediction equations and ground motion prediction equations

a) b)

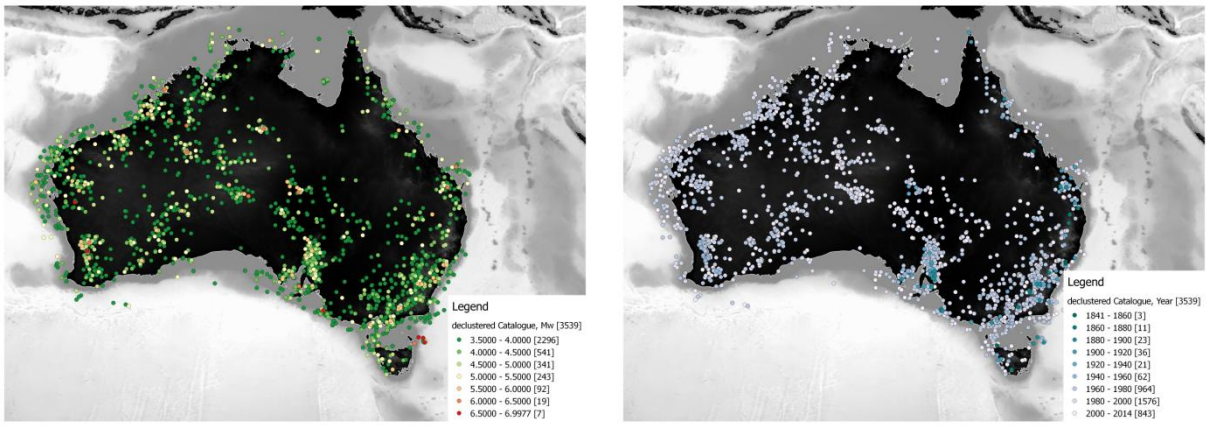

Figure 4: Earthquake distribution for Mw ≥ 3.5 for the applied declustered catalogue, using the procedure of Gardner and Knophoff, [1974]: a) earthquake distribution by moment magnitude, b) earthquake distribution by year.

4.1 Data

Multiple data sources have been used to establish an extended view of Australia's earthquake hazard. For earthquake data the official earthquake database of Geoscience Australia was used, implementing all earthquakes. After conversion, with a minimum magnitude of Mw ≥ 2.0, this catalogue contains about 14320 events since 1897. Additionally, the historical earthquake data of McCue et al. [2002] extended the catalogue with 73 additional earthquakes from 1840 to 1950, which are not part of the main data set. Furthermore, the Australian earthquake fault plane solution catalogue [Leonard et al., 2002] was used to gain spatial data about earthquake rupture orientation. For the modelling of seismic zones multiple versions have been developed and tested with respect to the effects on the Gutenberg-Richter distribution and seismic similarities. For the final model, a geometry whose spatial extent follows roughly Australia's crustal elements [Shaw et al., 1996] has been considered most promising to model seismic zones. The earthquake data has been declustered in two different ways. At first a standard window method has been applied as was used in Section 3, reducing the catalogue to 3539 events with a minimum magnitude of 3.5. This declustered set of earthquakes will be subsequently used to calculate the Gutenberg-Richter relation parameters. In addition, the complete dataset has been declustered a second time using an optics-based cluster method based on Ankerst et al. [1999], which will be further explained in the following section. The optics-declustered data are used to identify the distribution of background seismicity.

4.2 Clustering

The Optics-cluster method originates from the field of big data analysis to identify data correlations via clustering. For the alternative hazard model, the Optics cluster method is applied in two ways; once to generally decluster the earthquake catalogue and additionally to identify spatio-temporal clusters and respective parameters, e.g. cluster orientation to infer fault rupture information. The algorithm searches the neighbourhood of each data point and connects spatio-temporal neighbours into a cluster, while differing between border points (points within a certain distance) and core points (points surrounded by a minimum number of border or other core points). The cluster search starts always from core points. If a point is surrounded by a minimum number of points N_{min}, the point is set to be a core point, and each of the surrounding points are either core points or boundary points, depending on how many further points are around. Only the neighbourhoods of core points are investigated. For

analyzing earthquake clusters $N_{min} = 5$, each data point can only be assigned to one cluster. The neighbourhood in space is defined by $\varepsilon_s\ (M_w)$ and for time by $\varepsilon_t(M_w)$:

$$\varepsilon_s\ (M_w) = MAX(MIN(10^{0.25*M_w+0.5}; 150); 25) \tag{4.1}$$

$$\varepsilon_t\ (M_w) = MAX(MIN(10^{0.6*M_w-0.5}; 2400); 30) \tag{4.2}$$

For declustering, all data points are analyzed with respect to their neighbourhood and assigned to respective clusters. All points which are part of clusters larger than 10 elements are removed except for the point with the largest magnitude, which is thus assumed to be the main show and all other earthquakes are fore- or aftershocks. The remaining events are assumed to represent the background seismicity. The second application of the cluster method identifies the spatial pattern of each single cluster. Therefore, the cluster size has to be larger than 10 events. The spatial distribution is approximated by a 2D-Gaussian from which the major cluster angle is calculated if the directional unconformity is larger than 10%. Each cluster is afterwards stored by size, location and inclination. Based on the full earthquake dataset of Australia, 213 separate clusters have been identified.

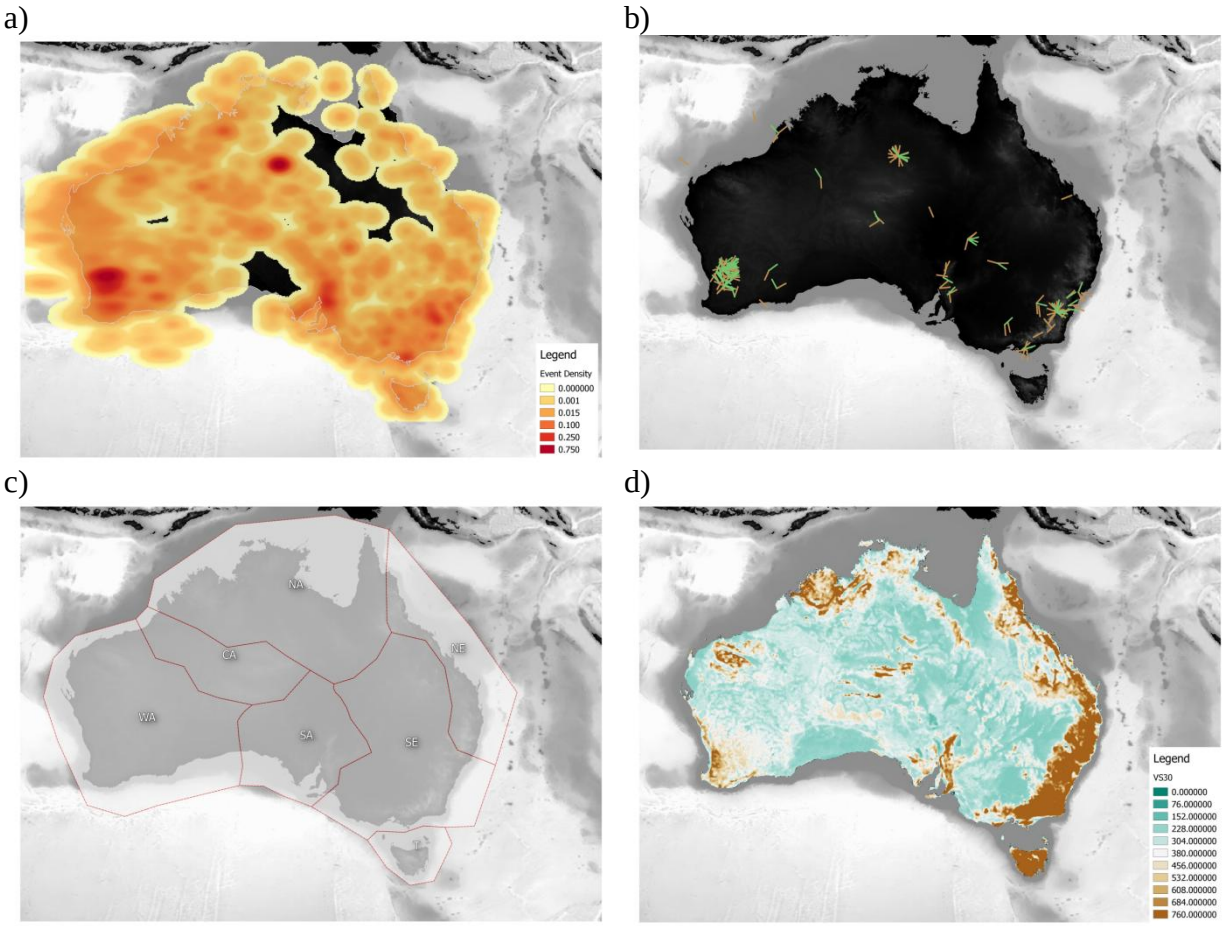

Figure 5: a) Smooth seismicity map of Australia, based on an Optics-declustered dataset, representing the estimated background seismicity. b) combined map of fault planes, based on cluster analysis (green) and fault plane solutions (brown). c) Seismic zone map of Australia, following respective crustal zones. WA = Western Australia, CA = Central Australia, SA = South Australia, NA = North Australia, NE = North-East Australia, SE = South-East Australia, T = Tasmania. d) VS30 model of USGS (see acknowledgement) in m/s.

4.3 Stochastic Hazard Model

The stochastic model, like the official Australian hazard map of 2012, uses a zone model to identify seismic locations. Instead of using a multilayer model, 8 seismic provinces will be

applied, which are based on the crustal elements identified by Shaw et al. [1996]. The overall b-value was estimated to be about 1.013. In total, 8 seismic zones have been modelled, shown in Figure 6. Most of the zones tend to have small b-values, which are undeniably related to the short time period of available data. The completeness has been estimated using an expert opinion approach by comparing the settlement history of the difference source zones with the possibility of recording an earthquake of a specific magnitude. For example, the completeness for magnitude 6-7 events for South-East Australia coincides with the founding year of Sydney. Independent of the zone-dependent Gutenberg-Richer analysis, the background seismicity has been estimated using the optics-declustered data. The background seismicity is used to model the spatial distribution of earthquakes; thus a smooth seismicity map has been developed. A spatial grid with a size of 10x10 km² has been applied using a Gaussian smoothing algorithm with a smoothing distance of 50 km. Afterwards, to avoid extreme localization due to remaining hotspots, each grid value was taken by its power to 0.75, then grid points with more than 75% of the maximum density value were capped to 75% of this respective value. To account for unknown seismicity in quiet regions, the smallest non-zero density was set for empty regions. The resulting smooth seismicity map is shown in Figure 5.

ID	**T**	**WA**	**CA**	**SA**	**NA**	**NE**	**SE**
#events	50	753	384	580	445	146	938
a-value	2.01	4.86	4.08	4.62	4.24	3.38	5.42
b-value	0.61	1.01	0.91	1.04	0.91	0.87	1.20
Completeness							
Mw > 3.5	1970	1960	1970	1950	1970	1945	1950
Mw > 4.0	1945	1945	1965	1930	1965	1925	1935
Mw > 4.5	1915	1940	1945	1910	1965	1905	1905
Mw > 5.0	1850	1892	1920	1885	1920	1875	1875
Mw > 5.5	1804	1892	1880	1865	1900	1825	1835
Mw > 6.0	1804	1826	1880	1836	1870	1825	1835
Mw > 6.5	1804	1826	1880	1836	1870	1788	1788
Mw > 7.0	1804	1826	1880	1836	1870	1788	1788

Table 3: Overview of all source zone parameters, P=Perth, T=Tasmania, WA = Western Australia, CA = Central Australia, SA= South Australia, NA = North Australia, NE = North-East Australia, SE = South-East Australia.

Based on the cluster analysis and the fault plane solution catalogue [Leonard et al., 2012] 76 rupture lines from clusters and 119 from fault planes have been used to determine the preferred rupture orientation. Nevertheless, the uncertainties for rupture orientation are still quite large, except for the Flinders area and South-East Australia. However, in general there are barely any preferred locations indicated. Thus, for most of the cases, the preferred rupture orientation remains relatively arbitrary. The rupture length of each earthquake is based on the equations of [Leonard, 2010]. Following the description of [Burbidge, 2012] a linear combination of multiple ground motion prediction equations have been applied. Both Australian GMPE equations of Somerville et al. [2010] and Allen [2012] have been implemented together with the equations of Akkar and Bommer [2010] and Lin and Lee [2008]. Each equation is equally weighted, whilst the first two mentioned models account for the local setting of Australia. The model implements VS30 soil conditions to account for site effects.

The final results are given as peak ground acceleration (PGA). Two time periods have been considered, 500 years and 1000 years. To account for location uncertainties, 100 independent stochastic datasets have been modelled for each return period to account for location

uncertainty. The record of PGA for each set is combined via superposition, showing always only the maximum value per location, the mean and standard deviation. Afterwards, the PGA map is smoothed using a Gaussian smoothing algorithm. Figure 6 shows the final smooth PGA map in g = 9.81 m/s² for 500 year PGA modelling and also for a 1000 year modelling. The smoothing algorithm lowers the PGA values in the maps, especially in the near field of a rupture. Based on the local soil conditions, for a maximum PGA of up to 1.65 g have been observed in both models, these peaks have been smoothed out as described above. In case of the mean PGA, the unsmoothed data indicated an increase of about 10-20% with respect to local soil conditions.

a) maximum PGA, 500 years

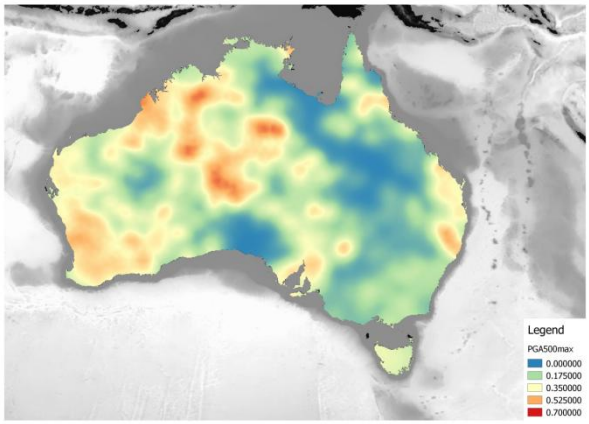

b) maximum PGA, 1000 years

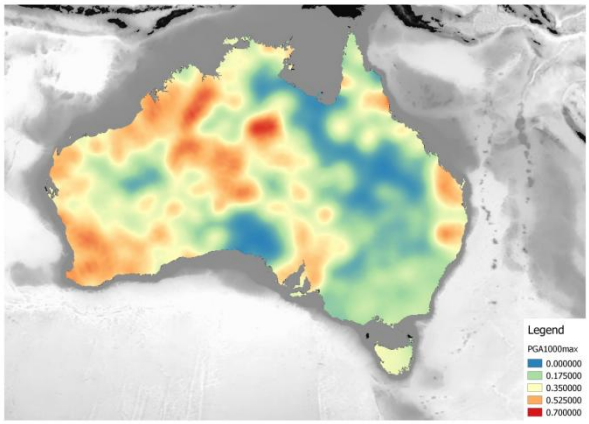

c) mean PGA, 500 years

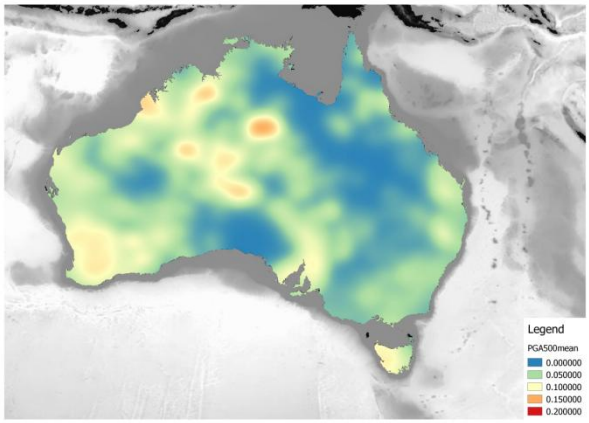

d) mean PGA, 1000 years

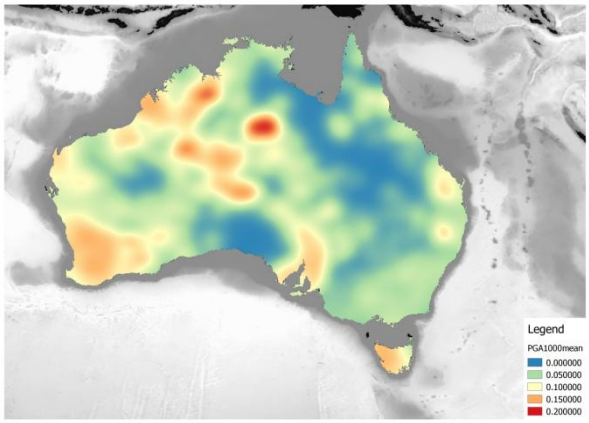

e) standard deviation of PGA, 500 years

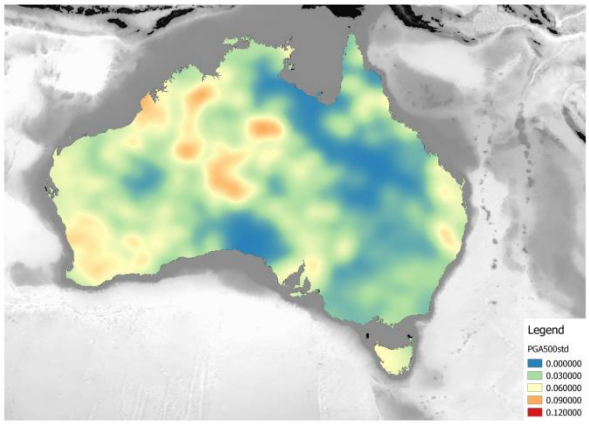

f) standard deviation of PGA, 1000 years

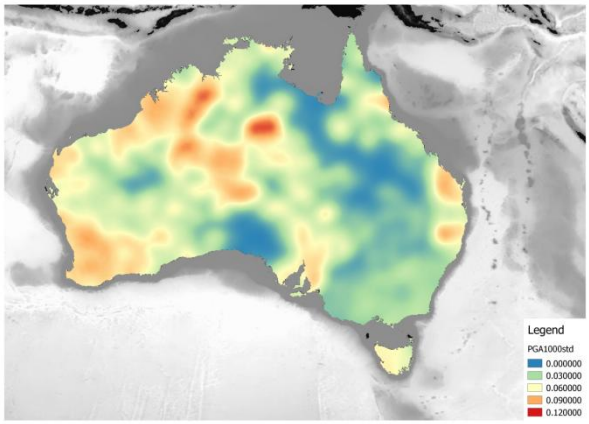

Figure 6: Superposition of 100 stochastic earthquake catalogues PGA models for 500 years [(a, c, e)] and 1000 years [(b), (d), (f)] show the respective smooth PGA maps, which are recommended as alternative hazard maps, with respect to maximum(a & b) and mean (c & d) PGA as well as standard deviation (e & f). Please note the changing colour index.

5. Results & Conclusion

Based on a direct comparison of the alternative hazard maps of this study to the original hazard map presented in Section 2, some extreme differences are observed. From the three maps per return period which are introduced in figure 6, the mean PGA map is advised to be seen as hazard map for design purposes with respect to the map of standard deviations. The maximum PGA map is advised as an indicator of the possible extreme. In general with respect to the original hazard map, the spatial distribution of more wide spread, especially in Western Australia and some more hotspots show up, for example along the eastern coastline. Furthermore, the overall expected mean PGA is about 20-50% higher than in the originally proposed version. This indicates an inherent threat for the communities of Melbourne, Sydney, Adelaide, Canberra, Perth and Brisbane. Especially Brisbane shows a tremendous increase of seismic hazard. The lower seismic hazard of Victoria and southern New South Wales is related to the extended data completeness regarding the historic record of possible strong earthquakes which might have been felt by the first settles. Since almost all observed seismicity is accounted as intraplate activity, there are no distinct fault-like features present. All locations which had seismic activity in the past might be prone for future activation. Implementation of historical data is extremely important; thus a lot of larger magnitude events did not show up in the original approach. The historical data is not considered to be totally reliable due to its spatial and temporal completeness and its scarcity, thus the major part of the data is still based on the observations since 1900. The changes to the magnitude frequency distribution related to the extended database and the altered seismic zone and spatial distribution model lead to an overall increase of earthquake hazard.

This alternative perspective for an Australian hazard map is evidently not as detailed as the official version, since distinct testing of ground motion equations, magnitude conversions, seismo-tectonic analysis etc. are acknowledged to be extremely time consuming. Instead, this study indicates future fields of investigation for a more in-depth analysis, which might also contain location specific timeline-analysis and additional tuning of the zones. However, using a more dynamic algorithm for earthquake distribution and historic earthquake data, even if it is extremely scarce, is highly recommended. For a location such as Australia with such a limited data background each additional piece of information can only improve future hazard models and make them more reliable.

Acknowledgements

Waveform data, metadata, or data products for this study were accessed through the Northern California Earthquake Data Center (NCEDC), here: earthquake data for Turkey. For visualization, SRTM digital elevation data has been used, respective [Jarvis et al., 2008].

References

AHEAD Working Group. AHEAD, the European Archive of Historical Earthquake Data, doi:10.6092/INGV.IT-AHEAD

Akkar, S., Bommer, J. J. 2010. Empirical equations for the prediction of PGA, PGV and spectral accelerations in Europe, the Mediterranean region and the Middle East. Seismological Research Letters, 81(2), 195–206.

Allen, T.I., 2012. Stochastic ground-motion prediction equations for southeastern Australian earthquakes using updated source and attenuation parameters, GA record 2012/69.

Ankerst, M., Breunig, M., Kriegel, H.-P., Sander, J., OPTICS: Ordering Points To Identify the Clustering Structure, Proc. ACM SIGMOD'99 International Conference on Management Data, Philadelphia PA, 1999

ANSS - Advanced National Seismic System - http://www.ncedc.org/anss/catalog-search.html

Burbidge, D. R. (ed.), 2012, The 2012 Australian Earthquake Hazard Map, Australian Government, Geoscience Australia, Record 2012/71, Geoscience Australia: Canberra

Elliot, J. R., Nissen, E. K., England, P. C., Jackson, J. A., Lamb, S. Li, Z., Oehlers, M., Parsons, B., Slip in the 2010-2011 Canterbury earthquakes, New Zealand, Journal of Geophysical Research, Vol. 117, B03401, doi: 10.1029/2011JB008868, 2012

Grünthal, G., Wahlström, R. (2012) The European-Mediterranean earthquake catalogue (EMEC) for the last millennium. Journal of Seismology 16(3): 535-570

Gardner, J. K., and L. Knopoff, (1974): Is the sequence of earthquakes in Southern California, with aftershocks removed, Poissonian?, Bulletin of Seismological Society of America, 64(5), 1363-1367

Geoscience Australia, Earthquake Database, http://www.ga.gov.au/earthquakes/searchQuake.do

Horton Jr., J. W., The 2011 Virginia Earthquake: What Are Scientists Learning? Eos, Vol. 93, No. 33, 317 - 324, 14 August 2012

Jarvis, A., Reuter, H.I., Nelson, A., Guevara, E., 2008, Hole-filled SRTM for the globe Version 4, available from the CGIAR-CSI SRTM 90m Database

Leonard, M., Ripper, I. D., Yue, L., 2010, Australian earthquake fault plane solutions, Geoscience Australia, Record 2002/19

Leonard M. 2010. Earthquake fault scaling; self-consistent relating of rupture length, width, average displacement and moment release. Bulletin of the Seismological Society of America 100, 1971-1988.

Lin, P.-S., & Lee, C.-T. 2008. Ground-motion attenuation relationships for subduction-zone earthquakes in northeastern Taiwan. Bulletin of the Seismological Society of America, 98(1), 220–240.

Schäfer, A., Daniell, J.E., Bunge, H.-P. , State-of-the-Art Review of Earthquake Forecasting Algorithms, Geological Society of Australia, 2014 Australian Earth Sciences Convention (AESC), Sustainable Australia. Abstract No 03ISC-P01 of the 22nd Australian Geological Convention, Newcastle City Hall and Civic Theatre, Newcastle, New South Wales. July 7 - 10, pp. 289 - 290.

Shaw, R.D., Wellman, P., Gunn, P., Whitaker, A.J., Tarlowski, C., and Morse, M. 1996. Australian Crustal Elements based on the distribution of geophysical domains (1:5,000,000 scale map), Version 2.4 ArcGIS dataset. Geoscience Australia, Canberra

Somerville P., Graves R., Collins N., Song S. G., Ni S. and Cummins P. 2009b. Source and ground motion models for Australian earthquakes. Proceedings of the 2009 Australian Earthquake Engineering Society Conference, 11-13 December 2009, Newcastle.

Stein, S., Geller R. J., Liu, M, Why earthquake hazard maps often fail and what to do about it, Tectonophysics 562 - 563 (2012), 1 - 25, doi: 10.1016/j.tecto.2012.06.047